https://doi.org/10.17221/25/2019-RAE

Investigation of sectional operating elements for conveying agricultural materials

Roman Hevko[1], Roman Rohatynskyi[2], Myroslav Hevko[3], Oleg Lyashuk[4], Oleksandra Trokhaniak[5]*

[1]*Department of Management of Bioresources and Nature Management, Faculty of Agricultural Economics and Management, Ternopil National Economical University, Ternopil, Ukraine*
[2]*Department of Economic Cybernetics, Faculty of Economics and Management, Ternopil Ivan Pul'uj National Technical University, Ternopil, Ukraine*
[3]*Technical department, Jinova s.r.o., Czech Republic*
[4]*Department Automobiles, Faculty of Engineering of Machines, Structures and Technologies, Ternopil Ivan Pul'uj National Technical University, Ternopil, Ukraine*
[5]*Department of Engineering Reliability, Faculty of Design and Engineering, National University of Life and Environmental Sciences of Ukraine, Kyiv, Ukraine*

Corresponding author: klendii_o@ukr.net

Citation: Hevko R., Rohatynskyi R., Hevko M., Lyashuk O., Trokhaniak O. (2020): Investigation of sectional operating elements for conveying agricultural materials. Res. Agr. Eng., 66: 18–26.

Abstract: The paper covers the results of the theoretical and experimental investigation of the developed sectional operating element of a flexible screw conveyer designed for transporting bulk agricultural materials. In order to determine the correlation between the design parameters of the hinged screw sections and the minimum permissible radius of curvature of a processing line, the analytical dependences have been deduced. The results of the experimental studies aimed at determining the efficiency of a screw conveyer and the level of the grain material damage depending on the change in design, kinematic and technological parameters of an operating element are presented.

Keywords: screw element; curvilinear line; conveyer efficiency; grain material damage; technological parameter

The set of requirements for conveying agricultural materials is, namely: the minimum energy costs needed for the material transportation, the processing reliability, the mobility of loading and unloading operations, the maximum efficiency of the material transportation as well as the minor damage of the bulk materials that are aimed to be used in their initial form (grain materials, granulated mineral fertilisers, etc.).

The research from Baranovsky et al. (2018) shows that the transportation of bulk materials by pneumatic conveyers with high processing mobility and efficiency is characterised by high energy costs that exceed similar screw conveyer data, which indicates the inexpediency of their application in small-scale mechanisation.

Several investigations have been conducted recently in order to improve the efficiency of rigid screw conveyers. The paper by Hevko et al. (2018) covers the improvement in the performance reliability of such conveyers by means of combining screw operating elements with safety units.

The process modelling of the bulk material transportation and the determination of the optimal parameters and operating modes of screw conveyers with their various arrangements are presented in

https://doi.org/10.17221/25/2019-RAE

the papers (Schlesinger et al. 1997; Merritt 2008; Lyashuk et al. 2015; Roberts et al. 2015; Rogatynska et al. 2015; Rohatynskyi et al. 2016; Sun et al. 2017).

In order to decrease the level of the bulk material damage, elastic elements are suggested to be used on a working helical surface, Tian et al. (2017). The papers (Zareiforoush et al. 2010; Hevko 2013; Špokas et al. 2016) cover the problem of a decrease in the level of grain material damage as well.

The determination of the optimal design parameters of loading hoppers and screw conveyer pipes as well as the operational modes of screw conveyers are presented in the papers (Klendii 2007; Fernandez et al. 2011; Li et al. 2013; Hevko et al. 2016).

Theoretical and experimental investigations aimed at determining screw conveyer efficiency are covered in the papers (Roberts et al. 1999; Owen et al. 2010).

According to the recent research (Hevko 2013; Hevko et al. 2016), the level of grain material damage in the process of its transportation by flexible screw conveyers is lower compared to its transportation by rigid screw conveyers. It can be explained by the fact that, in rigid screw conveyers, there is a uniform clearance between the torque screw and the fixed internal surface of a guiding casing and, if particles get into it, they become damaged. In flexible screw conveyers, an operating element is freely located in an elastic guiding casing and, when it rotates at more than 450 rev·min^{-1}, it is self-centred in its material flow and can be displaced in the radial direction of a casing, which provides a decrease in the level of bulk material damage. Here, the mobility of such conveyer types that can convey bulk materials along curvilinear routes is provided by changing the unloading area, thus having a stationary area of the bulk material loading. In order to increase the operating life of screw operating elements, it is suggested to make them sectional and hinge-jointed, according to the principle presented in the paper by Hevko et al. (2017).

Based on the analysis of known studies, it can be concluded that a comprehensive solution to the problem of improving the performance of flexible screw conveyors, which is to reduce the material consumption of the working bodies, ensuring optimal performance while minimising the degree of damage to the transported bulk materials, needs improvement and new research.

The aim of the research is to improve the performance of the developed screw operating element of a flexible screw conveyer by means of determining its optimal parameters and operating modes.

MATERIL AND METHODS

Determining the dependence of the minimum radius of the line curvature on the parameters of an operating element. In order to improve the flexible screw conveyer performance, a hinged sectional screw operating element was developed by Hevko (2013). The element makes it possible to convey bulk materials along curvilinear routes. Its design is presented in Figure 1.

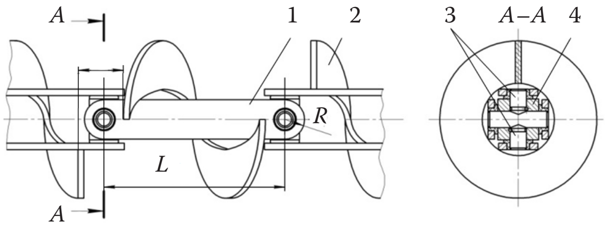

Figure 1. Design of a sectional screw operating element and section A-A

1 – plates; 2 – spiral rib; 3 – cylindrical radial pins 4 – square base; L – the length of the section of the screw working body; R – the radius of the side plates

While in operation, the screw operating element rotates in an elastic casing and conveys materials to an unloading area. The torque between the sections is transmitted through plates (1), where there is a spiral rib (2) mounted rigidly on a pair of cylindrical radial pins (3) and a square base (4). While the conveyer operates along the curvilinear routes, the plates rotate relative to the pins providing the torque transmission and material transportation by means of the spiral ribs. The spiral ribs of the adjacent sections are arranged with clearance .

The design of the flexible screw conveyer is presented in Figure 2. There is a re-loading pipe (1), which fits a loading line (2) in its top part and an unloading one (3) in its bottom part (Figure 2A) and a clutch (4) to provide rotation of the operating elements from an electric motor (5). The lines were made in the form of flexible casings, where the screw operating elements are arranged. The bulk material is poured out from a loading pipe to an unloading one in a re-loading pipe area.

The theoretical calculation was aimed at determining the relationship between the design parameters of the adjacent screw sections and the minimum permissible radius of the line curvature .

For this purpose, let us apply the analytical model presented in Figure 3. Figure 3A shows the arrangement of the sections in the XOY plane and Figure 3B

https://doi.org/10.17221/25/2019-RAE

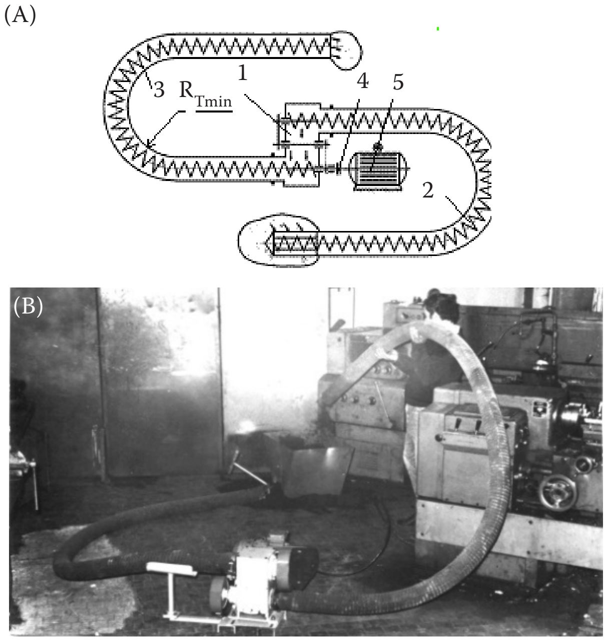

Figure 2. (A) The design of a flexible screw conveyer driven by an electric motor and (B) the general view of a conveyer

1 – loading pipe; 2 – a loading line 3 – an unloading line 4 – a clutch 5 – an electric motor

shows their arrangement in the mutually perpendicular X*O*Z plane.

When calculating, according to the technological effectiveness, the section framing was made of two flat parallel plates being *H* in width, the lateral surfaces of which were *R* in radius. The amount of clearance at the axial (initial) arrangement of the adjacent sections between their plates was equal to Δ_c.

It is necessary to determine the boundary values of the angles of the section turn, at which there is plane interaction that limits the minimum radius of the line curvature. For this purpose, conditionally, the left section (1) was arranged to be fixed and parallel to the *OX* axis. As for the right section (2), it was first rotated in the *XOY* plane and then in the *XOZ* plane.

Let us determine the minimum angle of turn (position of section 2^2 relative to section 2^1), at which the adjacent sections come in contact at point a in the projection on the XOY plane.

$$\varphi_{min} = \text{arctg}\left(\frac{\Delta_c}{R}\right) \tag{1}$$

where: *R* – the radius of the side plates; Δ_c – the size of the gap at the axial (initial) location of adjacent sections between their plates

Let us proceed to the projection *XOZ* (Figure 3B). When rotating the plates of section (2) relative to point *O*

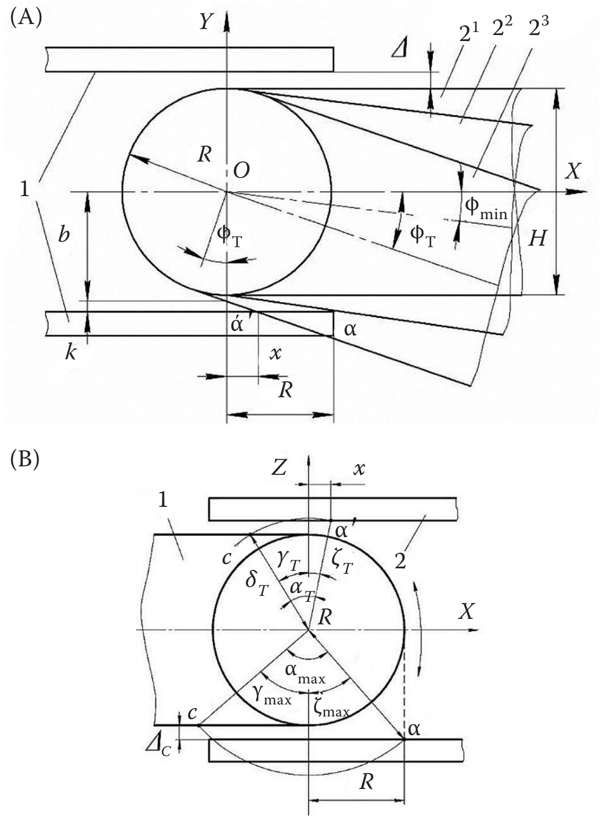

Figure 3. The scheme of the calculation of the design parameters of a hinge joint of the adjacent sections of an operating element. The (A) front and (B) side view

1 – left section; 2 – right section; *R* – the radius of the side plates; *O* – the center of the section rotations; *H* – width of section plates; *b*– the distance from the center of rotation of the side plate to its intersection with the axis OY; *k*– the size of the gap from the point of intersection of the side plate with the axis OY to the inner plane of the adjacent perpendicularly located side plate; α– the angle of rotation of the sections in the plane XOZ; φ_{min}– the minimum angle of rotation of the section 2; φ_T – the running angle of section rotation 2; γ_T – the angle between the line connecting the center of rotation of the side plate with the point c and the axis OZ at the top of it; ζ_T – the angle between the line connecting the center of rotation of the side plate with point a 'and the axis OZ at the top of it; Δc – the size of the gap at the axial (initial) location of adjacent sections between their plates; c – points of possible contact of adjacent side plates; *δ* – the section rotation radius 2

in a clockwise direction, point, with the turning radius , moves to point , which corresponds to the actual contact of the sections. This turning sector determines the maximum permissible angle of the section's rotation α_{max} in the *XOZ* plane at the set value of φ_{min}.Angle ζ_{max} is determined as follows (Equation 2):

https://doi.org/10.17221/25/2019-RAE

$$\zeta_{max} = \text{arctg}\left(\frac{R}{(R+\Delta_c)}\right) \quad (2)$$

where: ζ_{max} – maximum possible angle between the line connecting the center of rotation of the side plate with the point c and the axis OZ at the bottom of it; for more explanation see Equation (1).

In order to calculate γ_{max}, let us previously determine the value of δ (Equation 3):

$$\delta = \sqrt{2R^2 + 2R\Delta_c + \Delta_c^2} \quad (3)$$

where: δ– the section rotation radius 2; for more explanation see Equation (1).

Then Equation 4:

$$\gamma_{max} = \arccos\left(\frac{R}{\sqrt{2R^2 + 2R\Delta_c + \Delta_c^2}}\right) \quad (4)$$

where: γ_{max}– the maximum possible angle between the line connecting the center of rotation of the side plate with point a and the axis OZ at the bottom of it; for more explanation see Equation (1).

The next step of the calculation is the determination of the analytical dependences that relate to the current angle ϕ_T ($\phi_T > \phi_{min}$) to the current angle α_T ($\alpha_T > \alpha_{max}$) and the design parameters of a hinge joint. Such dependences make it possible to determine the equal values of ϕ_T and α_T and afterwards determine the value of R_{Tmin}.

Let us consider the third position of the plates of section 2^3, at which they rotate in the *XOY* plane as well as in the *XOZ* plane until their contact at point ά. Let us previously determine the distance *x* from the point of intersection of the adjacent plates (point ά) to the *OY* axis.

The value of *k* is determined as follows (Equation 5):

$$k = R + \Delta_c - b \quad (5)$$

where: for explanation see Equation (1) and Figure 3.

The value of *b* is determined as follows (Equation 6):

$$b = \frac{R}{\cos\varphi_T} \quad (6)$$

where: for explanation see Equation (1).

Having substituted Equation (6) into Equation (5), we obtain Equation (7A).

On the other hand we have Equation (7B).

$$k = R + \Delta_c - \frac{R}{\cos\varphi_T} \quad (7A)$$

$$\text{tg}\varphi_T = \frac{k}{x} \quad (7B)$$

where: for explanation see Equations (1) and (5).

Then we have Equation (8):

$$x = \frac{R + \Delta_c - \dfrac{R}{\cos\varphi_T}}{\text{tg}\varphi_T} \quad (8)$$

where: ϕ_T – the flow angle of the section rotation 2; for more explanation see Equations (1) and (5).

In order to determine α_T, let us conditionally rotate section (2) in a counter-clockwise direction.

The dependences to determine angles ζ and γ_T take the following form (Equation 9):

$$\zeta_T = \text{arctg}\frac{x}{R + \Delta_c} \quad (9)$$

where: for explanation see Equations (1) and (8).

Having substituted Equation (8) into Equation (9), we obtain Equation (10):

$$\zeta_T = \text{arctg}\frac{R + \Delta_c - \dfrac{R}{\cos\varphi_T}}{\dfrac{R + \Delta_c}{\text{tg}\varphi_T}} \quad (10)$$

where: for explanation see Equations (1) and (8).

In order to calculate angle $\gamma_{T,}$ the value of δ_T should be previously determined (Equation 11):

$$\delta_T = \frac{R + \Delta_c}{\cos\zeta_T} \quad (11)$$

where: for explanation see Equations (1) and (8).

Then Equation (12):

$$\gamma_T = \arccos\frac{R}{\delta_T} = \arccos\frac{R\cos\zeta_T}{R + \Delta_c} \quad (12)$$

where: for explanation see Equations (1) and (8).

Thus, the functional connection between $\alpha_T = f(\phi_T; R; \Delta_c)$ is determined from the following set of equations (Equation 13).

Having been given the specific values of R and Δ_c and discretely substituting the angle γ_T (upward beginning from φ_{min}), firstly, ζ_T is determined, then γ_T is defined, taking ζ_T into consideration and then α_T is determined.

https://doi.org/10.17221/25/2019-RAE

$$\begin{cases} \alpha_T = \xi_T + \gamma_T \\ \gamma_T = \arccos \dfrac{R\cos\zeta_T}{R + \Delta_{\tilde{c}}} \\ \xi_T = \text{arctg} \left\{ \dfrac{\dfrac{R + \Delta_{\tilde{c}}}{\cos\varphi_T}}{\left(R + \Delta_{\tilde{c}}\right) \times \text{tg}\varphi_T} \right\}. \end{cases} \quad (13)$$

where: for explanation see Equations (1) and (8).

Thus, for various values of R and Δ_c it is possible to set equal values of α and φ, which determine the inter-rotational movements of the adjacent sections.

Applying the set of Equation (13), it is possible to determine the radius of R_{Tmin}. At the set length of an operating element section L (Figure 1), the radius of the line curvature R_{Tmin} (Figure 2) is calculated by the dependence given in Equation (14):

$$R_{T_{min}} = \frac{L}{2\text{tg}\dfrac{\alpha_T}{2}} \quad (14)$$

where: for explanation see Equations (1) and (8).

Experimental plant and experimental procedure. In order to conduct the experimental research, an experimental plant was developed and made. Its general view is presented in Figure 4. There is an electric motor (2) arranged on a base (1) with the function of longitudinal movement and fixation. It is connected to an intermediate shaft (3) by means of a belt-and pulley drive. The torque is transmitted by means of a chain drive (4) from the intermediate shaft to the drive shaft of a screw operating element, which is located in a re-loading pipe (6) and an elastic casing (7). At the top of a pipe the hopper (5) is arranged.

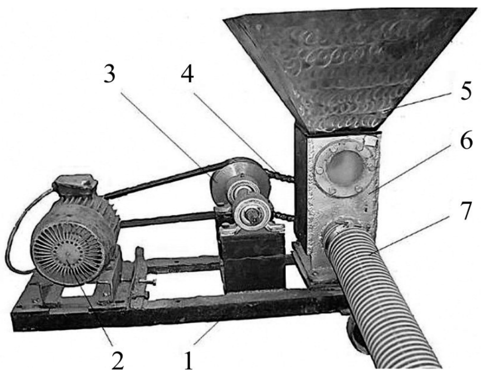

Figure 4. The general view of an experimental plant in a pushing mode of its operation

The presented version shows the pushing mode of the conveyer operation, that is to say, the bulk material moves from the drive shaft to an unloading area. In the pulling mode of the conveyer operation, the flap under the re-loading pipe opens and the frame is mounted on additional supports to provide the free spillage of the material at unloading. Here, an additional pipe hopper is mounted, where the loose end of a spiral is arranged.

The methodology for the experiment was as follows. Previously, grain has been poured into the bunker and transported to the unloading area. An Altivar 71 frequency converter (Altivar, France) and PowerSuite software (version 2.5.0) were used to start the engine and adjust its speed and, accordingly, the screw working body.

Procedure for determining the efficiency of a flexible screw conveyer. The experimental research was conducted using the plant presented in Figure 4. The parameters of the operating element were as follows: the internal diameter of the casing – 100 mm; the external diameter of the screw helix – 96 mm; the internal diameter of the screw helix – 46 mm; the helix pitch distance – 80 mm.

The casing spiral has been made of low carbon steel grade 0.8kp. The steel grade analogues are 0.8kp; on DIN – St12, St14; and on CSN – 11304, 11320, 11321.

A rubber-reinforced sleeve with an internal surface roughness has been used as the elastic casing $Rz = 40$.

The filling ratio of the conveyor technological line was within $K_T = 0.5–0.6$.

In order to investigate the conveyer efficiency, agricultural materials were used in the following bulk weight: wheat – 720 kg·m^{-3}; peas – 730 kg·m^{-3}; mixed feed – 550 kg·m^{-3}; bran – 250 kg·m^{-3}.

In order to determine the conveyer efficiency, a plant hopper was loaded with the bulk material. During the established stable transportation process (the casing is filled with material along the full length), the material was extracted into a measuring bin and the filling time was recorded. Then, the extracted material was weighed and its volume was measured. The investigations were conducted with a five-fold repetition.

Procedure for investigating the level of grain material damage. The laboratory investigation of the grain material damage depending on the design and kinematic parameters of a flexible screw conveyer was conducted the following way:

Prior to the grain material transportation, three samples of grain were taken. Then the number of

https://doi.org/10.17221/25/2019-RAE

damaged seeds was determined and the level of their damage was evaluated. The seeds with expelled kernels were not taken into account. Only the crushed seeds were considered. In determining the extent of the damage to the grain material, it has been transported 25 times by a developed screw working body in a flexible casing with a length of 4 m, which corresponded to 100 m of the total length of the transportation. The transported grain was backfilled into the bunker and transported to the unloading area.

The difference in the damage to the grain material before and after the transport cycle was to determine the degree of damage of the grain by sampling in a measured container. The experiments have been performed in triple frequency at different parameter values *n*, *m* and Δ.

According to the difference between the number of damaged seeds before and after their transportation, the level of grain material damage was determined depending on the change in the design and kinematic parameters of the operating element of the flexible screw conveyer.

RESULTS AND DISCUSSION

Results of theoretical investigations. According to the results of the analysis of Equations 13 and 14, Figure 5 presents the characteristic curves of the minimum permissible radius of the line curvature R_{Tmin} vs the value of the angular turn α_T of the adjacent sections at their various length L.

It has been determined that the size of the gap Δ_c is the dominant factor, in which the condition of the uniform turning of the sections is provided ($\phi_T = \alpha_T$) (Figure 3). Thus, a constant value of $R = 12$ mm for $\Delta_c = 0.5$ mm – $\phi_T = \alpha_T = 16.2°$; for $\Delta_c = 1$ mm – $\phi_T = \alpha_T = 22.2°$; for $\Delta_c = 2$ mm – $\phi_T = \alpha_T$ 1°; for $\Delta_c = 3$ mm – $\phi_T = \alpha_T = 36.6°$. The changing value of R at a constant value of Δ_c influences the change of the equal angles of ϕ_T and α_T to a less extent.

It has been determined that the dominant parameter that influences the minimum permissible radius of the line curvature R_{Tmin} is the amount of clearance between the plates of the adjacent sections.

It is important to mention that in order to provide the efficient operation of the flexible screw conveyer, it is necessary to increase the determined minimum permissible radius of the line curvature for 20–30% to guarantee the non-contact rotation of the hinged sections, which eliminates the possibility of emergency conditions and extends the operating life of the developed operating element.

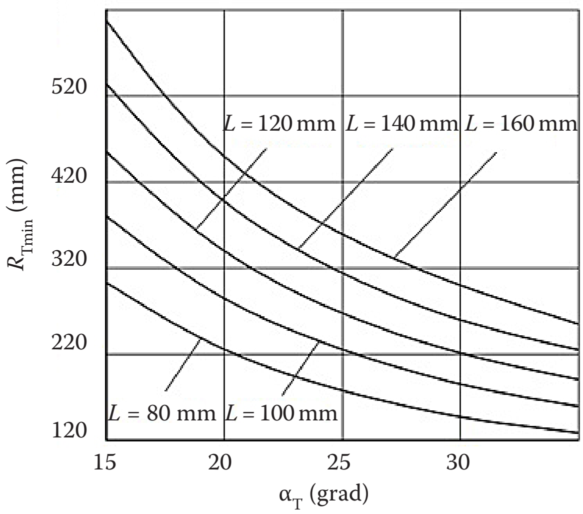

Figure 5. The minimum permissible radius of the line curvature R_{Tmin} vs the angle α_T characteristic curves

L – lenght; R_{Tmin} – minimum permissible radius of the line curvature; α_T –the value of the angular turn

Investigation results concerning the determination of the efficiency of a flexible screw conveyer. According to the results of the conducted investigation, Figure 6 presents the characteristic curves of the screw conveyer efficiency relative to the frequency of the operating element rotation when transporting various kinds of material.

Having analysed the curves, it can be said that the maximum conveyer efficiency when transporting materials of greater bulk weight (peas, wheat) is within the range of 650–670 rev·min^{-1} and their values are similar: (7– 7.2 m^3·h^{-1}; 5–5.2 t·h^{-1}). A further increase in the frequency of the operating element rotation results in a decrease in the conveyer efficiency, which can be explained by the smaller intake volume of the material that has a slower response at a greater bulk weight and is partially returned back to the hopper. As for light materials (mixed feed, bran), there is an increase in the productivity of the screw conveyor in the full range of the rotation frequency changes of the working body (540–790 rev·min^{-1}). In this case, the dependency characteristics of bran transportation is close to a linear one.

The given results can be used in choosing the container volume based on the time of the transportation of the various materials by the flexible screw conveyor.

Results of the experimental research on determining the level of grain material damage. Based on the conducted multi-factor experiment and hav-

https://doi.org/10.17221/25/2019-RAE

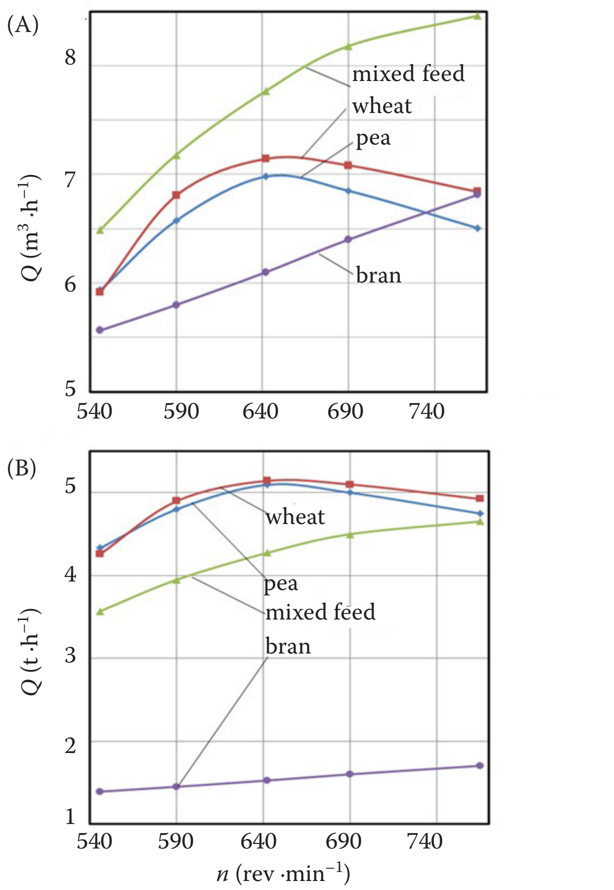

Figure 6. (A) The characteristic curves of volume and (mass) of the transported material per unit time vs (B) the rotation frequency of an operating element per unit time

ing processed the investigation results, a regression equation has been obtained for determining the influence of n, Δ and m (the mass of an operating element that was changed by means of applying sections of various length) on the level of grain material damage D (Equation 15).

The factorial field was determined by such a range of the parameter change: $450 < n < 750$ (rev·min^{-1}); $3.49 < m < 4.44$ (kg·lm^{-1}); $0.014 < \Delta < 0.042$ (m); lm – linear meter.

Figure 7 presents the response surfaces of the change in the level of D depending on simultaneous change of two factors: A – $D = f(m, n)$; B – $D = f(\Delta, n)$; C – $D = f(\Delta, n)$.

It has been determined that the dominant factors that influence the level of the grain material damage

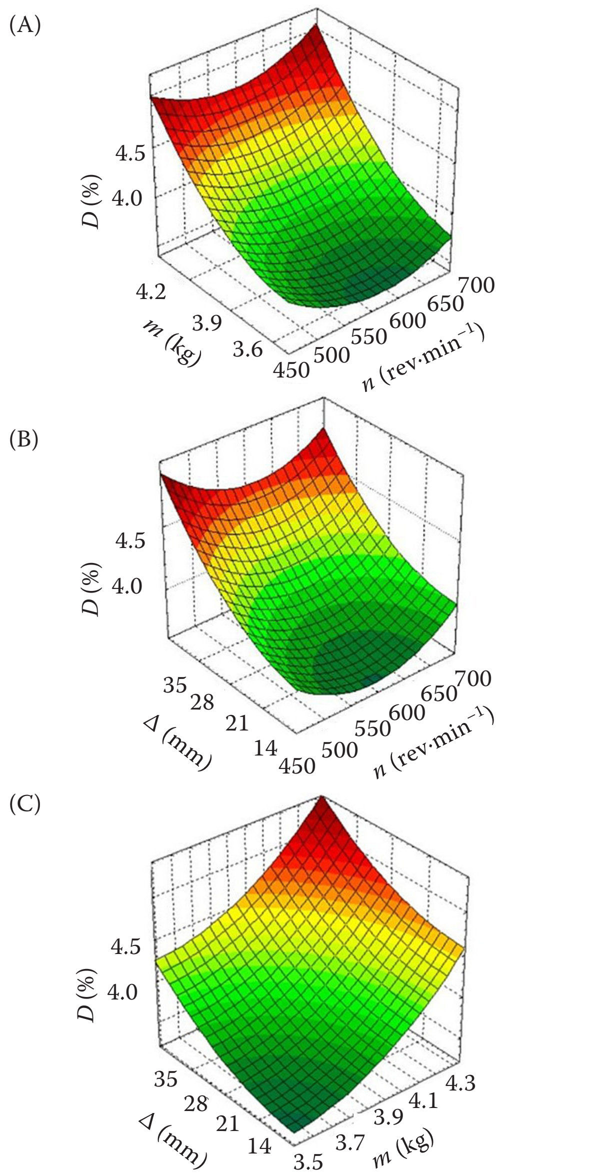

Figure 7. The response surfaces of the dependences: (A) $D = f(m, n)$ (B) – $D = f(\Delta, n)$ (C) – $D = f(\Delta, m)$

D is the amount of clearance Δ between the screw ribs of the adjacent sections (Figure 1).

When conducting the experimental studies to construct the regression equation 15 and its surfaces (Figure 7), the statistics data of the analysis of variance were as follows: the multiple determination coefficient – $D = 0.065$; the multiple correlation coefficient $R = 0.256$; Fisher's criterion $F = 1.750$; the probability coefficient of determination $P = 0.98042$.

$$D = 20.51 + 9.38 \times 10^{-4} n - 8.7m - 1.23 \times 10^{-2}\Delta - 8.98 \times 10^{-4} nm - 1.67 \times 10^{-5} n\Delta + 7.22 \times 10^{-3} m\Delta + 6.22 \times 10^{-6} n^2 + 1.22m^2 + 5.77 \times 10^{-4}\Delta^2 \quad (15)$$

where: D – the damage to grain material; n– screw speed rotation; m– the mass of the working body; Δ – the distance between the ends of the spiral adjacent sections.

https://doi.org/10.17221/25/2019-RAE

The analysis of the response surfaces (Figure 7) states that the increase in the linear mass of an operating element T leads to significant increase in the grain material damage D, the frequency of rotation of an operating element n has and the smallest influence. In addition, it can be said that at the frequency of rotation of an operating element being within the range of 550–650 rev·min^{-1}, there is the minimum level of grain material damage observed.

The theoretical and experimental research of the developed hinged connected sectional screw working body have made it possible to determine the optimum limits of its constructive and kinematic parameters for the efficient operation of the flexible screw conveyor.

Compared with pneumatic conveyors, the analysis and research, which are given in the following works (Hevko 2013; Baranovsky et al. 2018), and the proposed type of screw working body is characterised by 8–12 times lower energy consumption for the process of transporting the bulk materials.

Comparing the work of the hard (horizontal, inclined and vertical) screw conveyors whose research is described in the articles (Schlesinger et al. 1997; Merritt 2008; Lyashuk et al. 2015; Roberts et al. 2015; Rogatynska et al. 2015; Rohatynskyi et al. 2016; Sun et al. 2017), it can be stated that the proposed construction of the working body is distinguished by the fact that makes it possible to transport materials along curvilinear tracks, which significantly increases the performance of flexible screw conveyors.

The use of continuous flexible screw spirals is possible with a minimum radius of curvature in the technological line of about 1.5 m, because the smaller the radius of curvature of the spiral and as a result of alternating cyclic loads, they rapidly collapse (Hevko 2013; Hevko et al. 2016), while the proposed operating body can operate at the minimum radius of curvature in the technological line of about 0.5 m, (Figure 5), which significantly increases the mobility of the flexible screw conveyors.

CONCLUSION

To improve the operational performance of flexible screw conveyors, a hinged joint section screw working body has been developed. It allows the transportation of bulk materials along the curvilinear lines. Due to the use of hinge joints in the design of such a working body, its operational reliability and durability considerably increases in contrast to the continuous flexible screw working bodies, which are rapidly break while working on curved tracks due to the occurrence of alternating cyclic loads.

The article presents the experimental installation of a flexible screw conveyor on the given methods for determining the productivity of transporting various agricultural materials, as well as the degree of damage to the grain material.

On the basis of the conducted research, the functional dependences are deduced and the tabular data of the recommended ratios of the minimum radius of curvature of the technological line R_{Tmin} from the magnitude of the angular rotation a_T of the adjacent sections at different values of their length L are given in Table 1.

According to the results of experimental research, it has been determined that the maximum conveyer efficiency for transporting peas and wheat is within the range of n = 650–670 rev·min^{-1} and their values are similar: (7–7.2 m^3·h^{-1}; 5–5.2 t·h^{-1}).

The conducted research on determining the influence of the values of n, Δ, m on the level of the grain material damage D show that the values of Δ and τ are the dominant factors and the frequency of rotation of the operating element n has less influence. If the frequency of the operating element rotation is within the range of 550–650 rev·min^{-1}, there is minor damage to the grain material.

The use of the proposed sectional screw working bodies in the designs of flexible screw working bodies, taking the recommended parameters into account, will allow the efficient transport of agricultural materials along curvilinear tracks.

Table 1. Recommended ratio of the minimum radius of curvature of the production line

R_{Tmin} = 280 mm	R_{Tmin} = 330 mm	R_{Tmin} = 390 mm	R_{Tmin} = 460 mm	R_{Tmin} = 540 mm
$\alpha_T \le 26°$	$\alpha_T \le 24°$	$\alpha_T \le 22°$	$\alpha_T \le 20°$	$\alpha_T \le 18°$
L = 100 mm	L = 110 mm	L = 120 mm	L = 130 mm	L = 140 mm

R_{Tmin} – the radius of curvature of the process line; α_T – the flow angle of the sections in the plane XOZ; L – the length of the section of the screw working body

https://doi.org/10.17221/25/2019-RAE

REFERENCES

Baranovsky V.M., Hevko R.B., Dzyura V.O., Klendii O.M., Klendii M.B., Romanovsky R.M. (2018): Justification of rational parameters of a pneumoconveyor screw feeder, INMATEH: Agricultural Engineering, 54: 15–24.

Fernandez J.W., Cleary P.W., Mcbride W. (2011): Effekt of screw desing on hopper draw dawn by a horizontal screw feeder. In: Witt P.J., Schwarz M.P.: 7th International Conference on CFD in the Minerals and Process Industries CSIRO, Melbourne, Australia, Dec 9–11, 2011: 1–6.

Hevko M.R. (2013): Substantiation of the parameters of sectional screw conveyers for transporting loose agriculture materials, Ternopil, National Technical University: 178.

Hevko R.B., Rozum R.I., Klendiy O.M. (2016): Development of design and investigation of operation processes of loading pipes of screw conveyors. INMATEH: Agricultural Engineering, 50: 89–94.

Hevko B.M., Hevko R.B., Klendii O.M., Buriak M.V., Dzyadykevych Y.V., Rozum R.I. (2018): Improvement of machine safety devices. Acta Polytechnica, Journal of Advanced Engineering, 58: 17–25.

Hevko R.B., Yazlyuk B.O., Liubin M.V., Tokarchuk O.A., Klendii O.M., Pankiv V.R. (2017): Feasibility study of mixture transportation and stirring process in continuous-flow conveyors. INMATEH: Agricultural Engineering, 51: 49–59.

Klendii M.B. (2007): Substantiation of the parameters of a reloading branchpipe of a screw conveyer. Ternopil, National Technical University: 137.

Li H., Liu W. (2015): The Exprimental Research of Screw Conveyor Feeding System. In: Deng X., Dong X. (eds): New trends in mechanical engineering and materials, Book Series: Applied Mechanics and Materials, 251: 101–103.

Lyashuk O.L., Rogatynska O.R., Serilko D.L. (2015): Modelling of the vertical screw conveyer loading. INMATEH: Agricultural Engineering, 45: 87–94.

Merritt A.S. (2008): Mechanics of tunnelling machine screw conveyors: a theoretical model. Geotechnique, 58: 79–94.

Owen P.J., Cleary P.W. (2010): Screw conveyor performance: comparison of discrete element modelling with laboratory experiments. Progress in Computational Fluid Dynamics, 10: 327–333.

Roberts A.W. (1999): The influence of granular vortex motion on the volumetric performance of enclosed screw conveyors. Power Technology, 104: 56–67.

Roberts A.W. (2015): Bulk Solids: optimizing screw conveyors. Chemical Engineering, 122: 62–67.

Rogatynska O., Liashuk O., Peleshok T., Liubachivskyi R. (2015): Investigation of the process of loose material transportation by means of inclined screw conveyers. Bulletin of I. Pyliui Ternopil, 79: 137–143.

Rohatynskyi R.M., Diachun A.I., Varian A.R. (2016): Investigation of kinematics of grain material in a screw conveyor with a rotating casing. Bulletin of Kharkiv Petro Vasylenko National Technical Univarsity of Agriculture, 168: 24–31.

Schlesinger D., Papkov A. (1997): Screw conveyor calculation based on actual material properties. Powder Handling and Processing, 9: 321–325.

Špokas L., Adamčuk V., Bulgakov V., Nozdrovický L. (2016): The experimental research of combine harvesters. Research in Agriculture Engineering, 62: 106–112.

Sun X.X.; Meng W.J., Yuan Y. (2017): Design method of a vertical screw conveyor based on Taylor-Couette-Poiseuille stable helical vortex. Advances in Mechanical Engineering, 9: 1–11.

Tian Y., Yuan P., Yang F., Gu J., Chen M., Tang J., Su Y., Ding T., Zhang K., Cheng Q. (2018): Research on the principle of a new flexible screw conveyor and its power consumption. Applied Sciences, 8: 1038–1052.

Zareiforoush, H., Komarizadeh, M.H., Alizadeh, M.R. (2010): Effect of crop-screw parameters on rough rice grain damage in handling with a horizontal screw conveyor. Journal of Food, Agriculture and Environment, 8: 494–499.

Recieved: March 25, 2019
Accepted: March 10, 2020
Published online: March 25, 2020